

# Variability in Tree-ring Width and NDVI Responses to Climate at a Landscape Level

Jiří Mašek,\* Jan Tumajer, Jelena Lange, Ryszard Kaczka, Petr Fišer, and Václav Trembl

Department of Physical Geography and Geoecology, Faculty of Science, Charles University, Albertov 6, 128 43 Prague, Czech Republic

## ABSTRACT

Inter-annual climatically driven growth variability of above-ground biomass compartments (for example, tree stems and foliage) controls the intensity of carbon sequestration into forest ecosystems. However, understanding the differences between the climatic response of stem and foliage at the landscape level is limited. In this study, we examined the climate-growth response of stem and leaf biomass and their relationship for *Pinus sylvestris* (PISY) and *Picea abies* (PCAB) in topographically complex landscapes. We used tree-ring width chronologies and time series of the normalized difference vegetation index (NDVI) derived from high-resolution Landsat scenes as proxies for stem and leaf biomass, respectively. We then compared growth variability and climate-growth relationships of both biomass proxies between topographical categories. Our results show that the responses of tree rings to climate differ

significantly from those found in NDVI, with the stronger climatic signal observed in tree rings. Topography had distinct but species-specific effects: At moisture-limited PISY stands, stem biomass (tree rings) was strongly topographically driven, and leaf biomass (NDVI) was relatively insensitive to topographic variability. In landscapes close to the climatic optimum of PCAB, the relationship between stem and leaf biomass was weak, and their correlations with climate were often inverse, with no significant effects of topography. Different climatic signals from NDVI and tree rings suggest that the response of canopy and stem growth to climate change might be decoupled. Furthermore, our results hint toward different prioritizations of biomass allocation in trees under stressful conditions which might change allometric relationships between individual tree compartments in the long term.

Received 21 June 2022; accepted 8 January 2023;  
published online 26 January 2023

**Supplementary Information:** The online version contains supplementary material available at <https://doi.org/10.1007/s10021-023-00822-8>.

**Author contributions:** J.M. conceived of or designed study, contributed new methods or models, performed research, analyzed data, and wrote the paper. J.T. contributed new methods or models and wrote the paper. J.L. contributed new methods or models and wrote the paper. R.K. contributed new methods or models and wrote the paper. P.F. performed research and analyzed data. V.T. conceived of or designed study, contributed new methods or models, and wrote the paper.

\*Corresponding author; e-mail: jiri.masek@natur.cuni.cz

## HIGHLIGHTS

- Tree rings showed a stronger climatic signal than NDVI
- Response of tree rings differ from NDVI for *P. abies*
- Coherent tree rings and NDVI of *P. sylvestris* strongly influenced by topography

## INTRODUCTION

Carbon sequestration in terrestrial ecosystems exhibits high inter-annual variability that depends on weather conditions (Anderegg and others 2012). This variability represents a significant uncertainty in global carbon cycle models (Le Quéré and others 2009; Pan and others 2011; Babst and others 2014). Carbon is stored in various segments of trees: For example, conifers in temperate forests sequester a large amount of carbon in stems (~ 45% of annually formed tree biomass), leaves (~ 15%), and the remaining about 40% are divided into roots (~ 25%) and branches (~ 15%) (Bernoulli and Körner 1999). Annual ring-width chronologies can be used to analyze the influence of climate on stem biomass formation (Girardin and others 2016, Babst and others 2017). Trends in leaf biomass can be assessed by remote sensing data, which are available for the entire Earth for recent decades at fine temporal and spatial resolution (Vicente-Serrano and others 2016; Song 2012).

Stem and leaf biomass increment tend to be correlated, which potentially allows linking information from both data sources (Babst and others 2018; Vicente-Serrano and others 2020). Vegetation greenness and leaf biomass represented by NDVI have been shown to correlate with tree-ring width and basal area increment (Vicente-Serrano and others 2016; Zhang and others 2018; Liang and others 2005; Schröder and Körner 2018; Berner and others 2013), wood density (Beck and others 2013; D'Arrigo and others 2000; Bunn and others 2013), earlywood and latewood width (Pompa-García and others 2021; Pasho and Alla 2015), seed production, apical increment (Wang and others 2004), and carbon isotope ratios in wood (del Castillo and others 2015; Leavitt and others 2008). On the other hand, this relationship may vary in time, space, and along various environmental gradients. For instance, temporal variability in the relationship between radial growth and canopy conditions might be caused by extreme drought events, either through direct (Gazol and others 2018b; Kannenberg and others 2019) or legacy effects (Wu and others 2017; Anderegg and others 2015). On a global scale, the links between canopy conditions and radial growth were shown to systematically differ between bioclimatic zones (Wong and others 2021; Kaufmann and others 2008; Seftigen and others 2018; Bhuyan and others 2017; Bunn and others 2013).

At a landscape level, the terrain morphology may significantly modulate the link between radial growth and canopy dynamics (Wang and others

2021; Kannenberg and others 2019; Coulthard and others 2017) because it influences water balance and topoclimate (Vicente-Serrano and others 2012, Vicente-Serrano and others 2016). Tree growth and NDVI are influenced by topographical factors such as slope orientation and inclination (Montpellier and others 2018; Zhan and others 2012; Oberhuber and Kofler 2000), elevation (Ponocná and others 2016; Zhan and others 2012), solar radiation (Riihimäki and others 2017), and soil water availability (Rabbel and others 2018; Adams and others 2014; Del-Toro-Guerrero and others 2019). Additional factors driving the relationship between tree rings and NDVI include species composition (Berner and others 2011; Lopatin and others 2006), canopy age structure (Alla and others 2017; Bhuyan and others 2017; Correa-Díaz and others 2019), and phenology (Bhuyan and others 2017; Gazol and others 2018a). Despite all this knowledge, there is a lack of studies combining tree rings and NDVI analyses covering several distinct topographic features and investigating the influence of topography on the climatic signal and the relationship between NDVI and tree rings.

A combination of tree-ring and remote sensing data has been used before to reveal trends in ecosystem productivity, but solely at regional (Vicente-Serrano and others 2020; Xu and others 2019), or continental to global scales (Bunn and others 2013; Kaufmann and others 2008; Vicente-Serrano and others 2012). Accordingly, most studies used satellite data with large spatial coverage but a low spatial resolution from hundreds of meters to a few kilometers per pixel (Vicente-Serrano and others 2020; Wang and others 2004; D'Arrigo and others 2000). However, low spatial resolution masks potential differences at a landscape level (Bhuyan and others 2017; Berner and others 2011) which can be vital for determining forest response to climate change (Correa-Díaz and others 2019; Bhuyan and others 2017). Both forest mortality and growth trends preserve topographic patterns, which are averaged out in large-pixel scenes (Wang and others 2021; Bhuyan and others 2017).

In this study, we aim to compare climate signals in leaf biomass (represented by NDVI derived from high-resolution satellite data) and stem biomass (represented by tree rings) in topographically complex landscapes. For this purpose, we sampled 40 sites of *P. abies* and *P. sylvestris* in areas representing lowland and mountain forests of the temperate zone. We hypothesize that growth trends in wood and leaf biomass and their climatic responses are correlated. We further expect that the strength

of this relationship varies according to topography due to differences in moisture accumulation and the amount of incoming radiation.

## METHODS

### Study Areas and Study Species

*P. abies* (PCAB) and *P. sylvestris* (PISY) account for about 30% and 20% of the species composition in Central Europe, respectively (Spiecker 2000; Durrant and others 2016). PCAB is characterized by a shallow root system taking up moisture from upper soil horizons. This species naturally occurs in mountainous uplands with nutrient-poor soils where it forms dense stands. PISY is a light-demanding species with a deep rooting system and high ecological tolerance; hence, it primarily occupies less productive sites, where it forms open-canopy stands (Durrant and others 2016).

To represent typical areas with a prevalence of either PISY or PCAB forests, we selected two landscapes in Central Europe (Czech Republic)—Kokořínsko hills (dominated by PISY) and Šumava Mts. (dominated by PCAB) (Figure 1). The Kokořínsko hills are a topographically complex area (Figure 1) formed by sandstone rock massifs and dissected by narrow canyon-shaped valleys of approximately 100 m depth (Bína and Demek 2012). The highest peaks (614 m a. s. l.) are formed by volcanic intrusions and parts of consolidated sandstones (Ložek and others 2005). PCAB sites

were situated in the Šumava Mts. (elevation of the local highest peak is 1235 m a. s. l.) in a mountain landscape composed of old metamorphic rocks forming gently inclined slopes (Demek and others 1965). Slope inclination in Kokořínsko hills is variable (mean of 15°), which contrasts with Šumava Mts., where slopes are uniform with a mean inclination of 10° (Table S1). While Kokořínsko hills are located in the mild temperate zone with annual precipitation totals of about 500–650 mm and a mean annual temperature of 8 °C, Šumava Mts. are located in the wet temperate zone with annual precipitation totals of 1200 mm and a mean annual temperature of approximately 4 °C (Figure 1). Winter snow cover lasts for about 80 days in Kokořínsko hills and almost 160 days in Šumava Mts. (period 1961–2000; Tolasz and others 2007). Soils in both areas are typically nutrient-poor leptosols, podzols, and cambisols (Ložek and others 2005; Albrecht and others 2003).

### Sample Collection and Processing

We sampled 20 sites in each study area to cover the variability of the landscape in terms of moisture availability and solar irradiation, involving the following four categories: south-facing slopes, north-facing slopes, plateaus, and valley bottoms (further referred to as site categories; Figure 1). Each site category was represented by five sites in each study area. At each site, we delineated a circular inventory plot with a radius of 16 m to

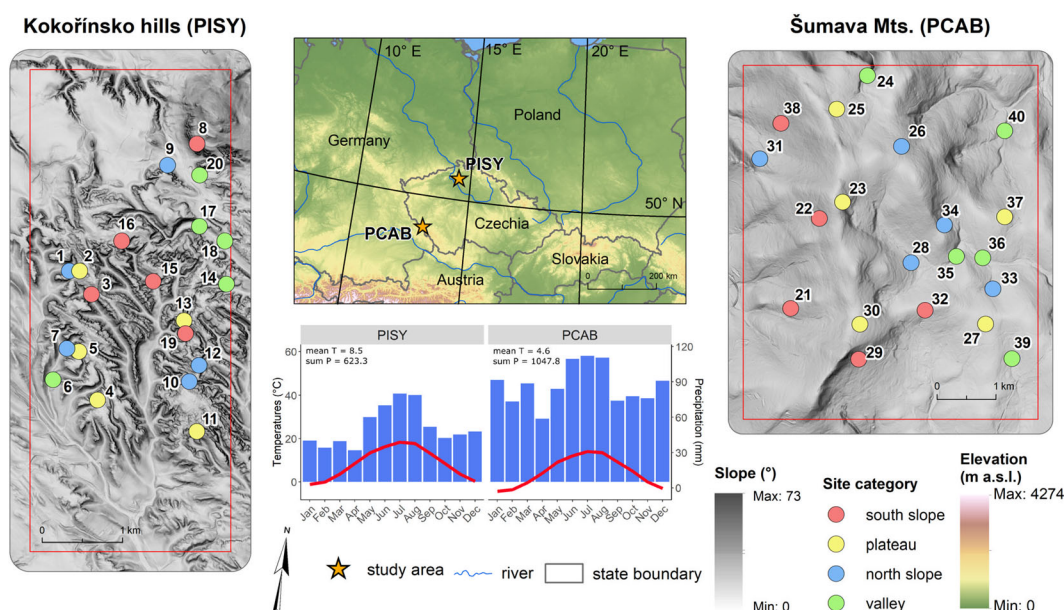


**Figure 1.** Study areas, location of sampled sites, and climate diagrams (1985–2017) for PCAB and PISY. Sites are numbered according to Table S2.

approximate the size of one pixel of the Landsat scene (30 m × 30 m). Plots were characterized by monospecific stands of the respective species. We sampled at least 26 canopy-level trees within each inventory plot using an increment borer. Additionally, at one site per each site category and species, we sampled all trees with a diameter at breast height (DBH) greater than 10 cm to consider the influence of tree age on the climatic response of tree compartments (Carrer and Urbinati 2004). Our dataset contains 1147 trees, 639 for PISY, and 508 for PCAB (Table S2).

Tree cores were dried, glued onto wooden laths, and sanded to improve the visibility of tree rings. Measuring tree-ring widths as a proxy for stem biomass increment was performed in WinDENDRO (Regent Instruments 2011) on scans with a resolution of 1200 dpi. Tree rings were automatically detected and then visually checked and corrected if necessary. We used PAST4 (Knibbe 2004) for cross-dating of the tree-ring series. Since we were interested in high-frequency variability, we removed age trends from individual series using a smoothing spline with a 50% frequency cutoff at a 30-year-long window. Tree-ring indices (TRI) were calculated as ratios of observed tree-ring width and the value predicted by the spline (Cook and Peters 1981). Because the detrending approach might influence the resulting climatic signal (D'Arrigo and others 2006), we also tested the trend removal using a spline with a 70-year-long window. The climatic signal was similar for both versions of the spline; therefore, all the following analyses were carried out using tree-ring series detrended with a 30-year-long window spline. Standard chronologies (Figure S1A) were built for each site using Tukey's Biweight Robust Mean in R (R Core Team 2019) and the package dplR (1.7.2; Bunn, 2008).

## NDVI Data

We used Landsat (high-quality T1\_SR scenes) satellite data to calculate NDVI (normalized difference vegetation index) as a proxy for leaf biomass for the window 1985–2021 (Shabanov and others 2005) because these data provide the longest currently available time series of multispectral scenes with high resolution (30 m per pixel since 1984) (Zhu and others 2018). Landsat 5, 7, and 8 are each using different sensors, TM (Thematic Mapper), ETM+ (Enhanced Thematic Mapper Plus), and OLI (Operational Land Imager), respectively, and they cover different time windows. Hence, datasets of Landsat 5 and 7 were recalculated by regression to be comparable with Landsat 8 (Roy and others

2016) by using Google Earth Engine (Gorelick and others 2017). We erased clouds and their shadows from all scenes to avoid distortion of spectral data (Zhu and others 2015). All available scenes for the growing season were selected. The start of the growing season for individual years was set to the first day in the year with a mean temperature of five preceding days over 12 °C, and 9 °C for PISY and PCAB, respectively, that is, mean temperature triggering bud burst reported for these species in a similar environment (Hájková and others 2012). The end of the growing season was set to 30th September (DOY 274), when trees in the temperate forests of Central Europe approximately complete their radial growth (Etzold and others 2021; Tumajer and others 2022; Krejza and others 2021). The leaf formation is usually completed before July with only limited subsequent changes in leaf biomass (Kraus and others 2016; Fajstavr and others 2019). Iterations with various lengths of the growing season revealed the negligible impact on climate-NDVI correlations. NDVI was calculated for each pixel of the selected scenes as follows:

$$NDVI = \frac{NIR - Red}{NIR + Red}$$

where 'Red' indicates reflectance in the red spectrum and 'NIR' refers to the reflectance in the near-infrared spectrum (NASA 2022). In the next step, the median NDVI from all scenes within the vegetation period was calculated for each year, and an annually resolved time series of these values was extracted for our sites. To relate these values to our study sites in the field, we computed the mean of all pixels overlapping with a respective study site (2 or 4 pixels in most cases) weighted by the proportion of sampling site area located inside a specific pixel.

Long-term trends in the time series of vegetation indices can be affected by various factors, including forest densification as trees are getting larger (Vicente-Serrano and others 2004) and CO<sub>2</sub> fertilization (Donohue and others 2013). To remove these trends, we fitted linear regressions to the NDVI time series and used the residuals for further analyses (Figure S2). Although our study sites are located in evergreen forests, the values of NDVI during the vegetation period in each year are slowly increasing and never reach full saturation (Figure S3).

## Climate Data

For both study areas, daily and monthly (Figure S1B) mean temperatures and precipitation to-

tals were obtained by interpolating data from the nearest meteorological stations of the Czech Hydrometeorological Institute. Stations with a maximum distance of 50 km from the sampling sites were considered for interpolation. The timespan of available climatic data covers the 1901–2018 period. Mean temperatures were interpolated by orographic regression, assuming the dependence of temperature on elevation (*R* package *gstat* 2.0–9; Pebesma 2004). Interpolation of precipitation was done using the inverse distance weighting method (Lu and Wong 2008). At least three stations were used to interpolate mean monthly temperatures and seven for precipitation, with an increasing number of stations over time. The standardized precipitation evapotranspiration index (SPEI, Vicente-Serrano and others 2010) was calculated in twelve different time steps with 1 to 12 considered preceding months in the calculation of the ratio between precipitation and evapotranspiration (*R* package *SPEI* 1.7; Beguería and Vicente-Serrano 2017). Evapotranspiration was computed using the Thornthwaite method (Thornthwaite 1948). We found that correlations between TRI or NDVI and the SPEI did not differ considerably between the various versions of SPEI. Therefore, we decided to use SPEI based on the four preceding months for final analyses since it was reported that SPEI 3–6 usually shows the best fit with NDVI (Vicente-Serrano and others 2012). SPEI 4 reflects a balance between deeply rooting species (PISY) which use water retained in the soil for most of the year, and shallow rooting species (PCAB), reaching soil layers with a relatively fast turnover of infiltrating water (Sprenger and others 2019).

## Statistical Analysis

All analyses were based on the time window 1985–2017 as the longest possible common period covered by TRI and NDVI data. Calculations were performed in *R* 4.2.0 (*R* Core Team 2022).

To assess the coherency of growth patterns, we employed a principal component gradient analysis (PCGA; *R* package *dendRolAB*; Buras and others 2016) for both TRI and NDVI. Using the 20 site chronologies per species, we determined the proportion of variability explained by the first principal component (PC1) as an indication of a common signal in the chronologies. We assumed that the second and third principal components (PC2 and PC3) capture growth variability attributed to the four site categories (valleys, plateaus, northern and southern slopes). Therefore, differences in loadings on PC2 and PC3 were tested between site categories

using ANOVA. Since there were significant differences in the age of trees between sites and site categories, we also ran a PCGA on a dataset containing solely adult trees with an age of 80–150 years. The results did not differ considerably; hence, all following analyses were carried out on the entire dataset.

To analyze climate-growth responses for each site, Pearson's correlations of TRI and NDVI with monthly mean temperatures and SPEI were computed. We included months that potentially have strong effects on tree growth, that is, the months from June of the year preceding tree-ring (leaf) formation until September of the ring-formation year (Fritts, 1976). We used the *R* package 'tree-clim' for dendroclimatic analysis (version 2.0.6.0; Zang and Biondi 2015). To examine how topography influenced the climatic signal in the TRI (as a proxy for stem biomass) and in the NDVI (as a proxy for leaf biomass) chronologies, differences in climate-growth correlations were compared between site categories using ANOVA. To assess similarities in climatic responses between TRI and NDVI from the same site category, we computed *t* tests of correlation coefficients between site categories and species.

To test how sensitivity to climate is influenced by topography, we calculated the correlation with the main driving variable for each site (for PISY mean SPEI from June to August, for PCAB mean SPEI of the previous year from June to August). Then, we fitted the linear model with climate-growth correlations (response variable) and altitude, slope, north deviation, and topographic wetness index (TWI; Beven and Kirkby 1979) as explanatory variables for each species and TRI and NDVI, respectively. Topographic variables were derived from LIDAR-based surface topography models with a regular grid of 5 × 5 m (DMR 4G; ČÚZK 2013) using ArcMap 10.7.1 (ESRI 2020). See Supplementary material for more information.

To quantify the relationship between wood and leaf biomass, we correlated the time series of TRI and NDVI for each site and tested differences in correlation coefficients between site categories using ANOVA.

## RESULTS

### Growth Variability Within TRI and NDVI

Growth coherency of both TRI and NDVI was strong: PC1 explained 58–74% of the variability between individual site chronologies both for PCAB and PISY. For PISY, the coherency was larger

for NDVI, while for PCAB, radial growth represented by the TRI was substantially more coherent than NDVI (Figure 2).

With respect to site categories, PCGA revealed significant differences for PISY TRI, clearly distinguishing plateaus and valleys (Figure 2A, Table S3) and between northern and southern slopes (Figure 2B). Valleys and northern slopes differed substantially, and plateaus and southern slopes revealed a nearly significant difference (Table S3). For PCAB, TRI and NDVI showed no systematic pattern and no significant differences between site categories along any PC (Figure 2).

### Topographic Variability in the Climatic Signal of TRI and NDVI

The climatic signal differed between biomass proxies, climate variables, species, and site categories. PISY TRI chronologies from plateaus showed the strongest correlations with both previous and current-year summer SPEI, followed by sites from southern and northern slopes, while responses in valleys were always weak and mostly insignificant (Figure 3). By contrast, the correlations of PISY TRI with temperature were strongest for valleys, followed by slopes, peaking from January to March of the current year. Plateaus showed non-significant or even significant negative TRI correlations with temperature during the previous June and December. Differences in climate-growth correlations between plateaus and valleys were

statistically significant for both temperature and SPEI in most tested months (Table S4). NDVI of PISY was mainly positively correlated with current-year summer SPEI (Figure 3). Plateaus and north slopes exhibited the strongest relationship with SPEI. Peak correlations of PISY NDVI with SPEI (culminating in current June and July) occurred about one month earlier compared to TRI (peak in current July and August). Relationships of NDVI with temperature showed two periods with statistically significant correlations: positive correlations with the previous October and negative correlations with March of the leaf-formation year.

PCAB TRI exhibited significant negative correlations with temperature in the previous summer and positive correlations with current January and March. PCAB TRI correlations with SPEI were mostly weak and insignificant (Figure 3). In contrast, NDVI was significantly negatively influenced by SPEI during the previous summer and autumn for all site categories. NDVI of PCAB revealed significant positive correlations with temperature during the previous August and December. Overall, there were no systematic differences caused by topography in the climatic signal of PCAB chronologies (Table S5).

Although the response of PISY TRI and NDVI to SPEI revealed very similar patterns (Figure 3), there were significant differences in absolute values of correlation coefficients. Specifically, the most prominent differences occurred for plateaus during the previous summer (correlations with TRI

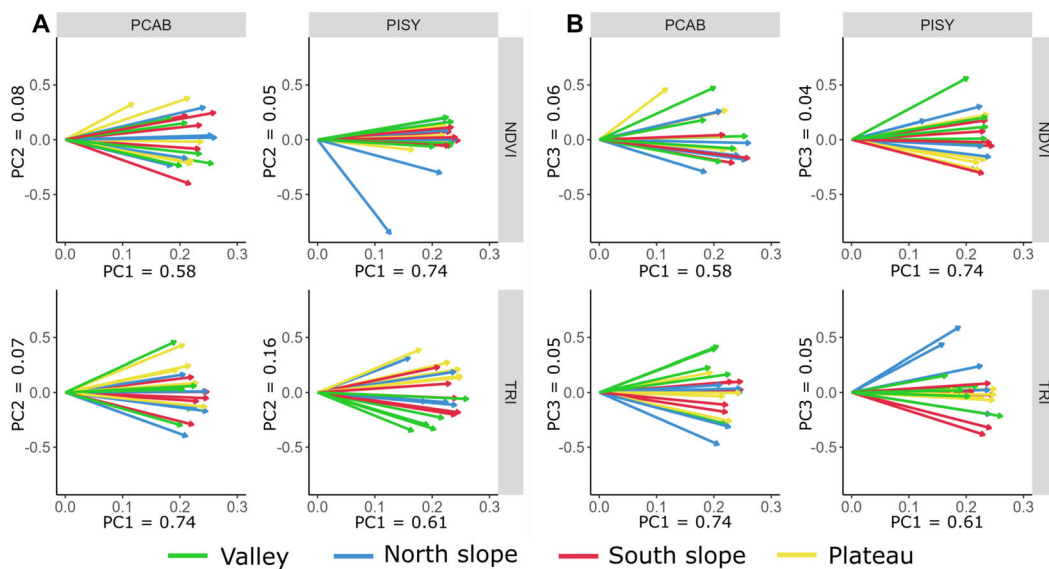


**Figure 2.** Biplots of principal component gradient analysis showing growth variability in TRI and NDVI time series covering the 1985–2017 period separately for PCAB and PISY sites. The color coding of site categories is indicated in the legend below. Panel A: PC1 versus PC2, panel B: PC1 versus PC3.

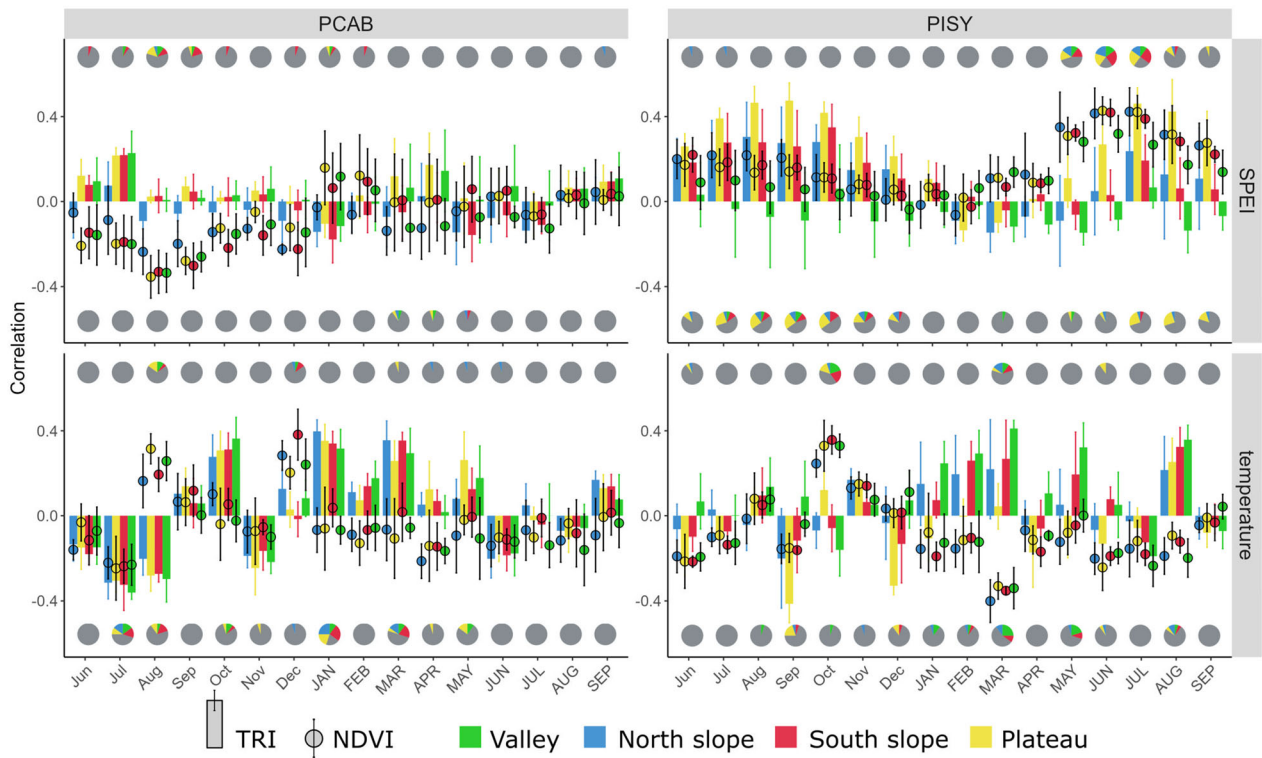


**Figure 3.** Mean correlations of TRI (bars) and NDVI (circles) with monthly mean temperatures (bottom) and SPEI (top) for PCAB (left) and PISY (right). Error bars show standard deviations between individual sites. Pie graphs denote the percentage of significant correlations observed for individual sites ( $p < 0.05$ ), upper row: NDVI, bottom row: TRI. The gray area represents non-significant correlations, and colors denote individual site categories (see legend below). Small letters indicate months of the previous year, and capital letters denote months of the current year.

stronger than with NDVI) and for valleys in the current spring (correlations with NDVI stronger than with TRI) (Table S6). For temperature, climate-growth correlations differed substantially between TRI and NDVI of PISY. There were opposite responses for TRI and NDVI, namely in the previous October (TRI negative, NDVI positive) and the current March (NDVI negative and TRI positive) (Table S6, Figure 3). For PCAB stands of all site categories, TRI and NDVI correlations with temperature and SPEI differed across almost all months of the previous year, winter, and spring of the ring-formation year (Table S6).

The linear model explaining correlations of PISY TRI with SPEI was statistically significant ( $R^2 = 0.85$ ,  $p$  value  $< 0.05$ ) with a strong influence of slope, TWI, and altitude on climatic sensitivity. A relatively high amount of explained variability ( $R^2 = 0.4$ ,  $p$  value = 0.09) was observed for a model explaining correlations of PISY NDVI and SPEI, where TWI revealed a significant effect. For PCAB both models were insignificant with a low coefficient of determination (Table S7).

### Relationship Between TRI and NDVI

Correlations between the time series of TRI and NDVI were statistically significant for 20% of the sites for PISY. Correlations were strongest for plateaus and generally decreased in the following order: south slopes, north slopes, and valleys (Figure 4). However, there was no statistically sig-

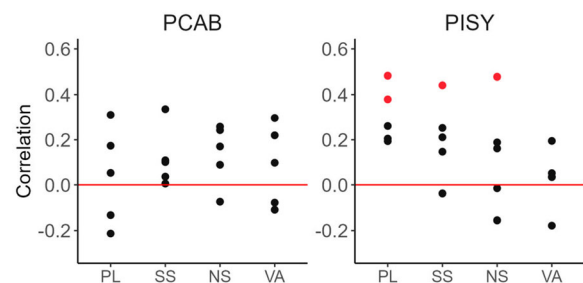


**Figure 4.** Correlations between TRI and NDVI chronologies per species and site category (SS—south slopes, NS—north slopes, PL—plateaus, VA—valleys). Red dots denote statistically significant correlations ( $p < 0.05$ ).

nificant difference between site categories with respect to mean TRI-NDVI correlations. For PCAB, all correlations between TRI and NDVI were non-significant.

## DISCUSSION

Our results highlight a complex pattern in climatic responses of tree-ring widths and NDVI that are driven by interactions of site climatic conditions, species, and topography. By combining analyses of tree-ring width (as a proxy for stem biomass) and NDVI (as a proxy for leaf biomass), we found that the climatic limitation of stem and leaf biomass can be significantly different close to a species' ecological optimum (our PCAB sites). On the other hand, climate-growth responses of tree rings and NDVI were more similar at the moisture-limited PISY sites, mainly for the SPEI drought index. Overall, the climatic limitation of tree rings was stronger and partly modulated by topographic conditions, while NDVI was less affected by topography in our study.

### Growth Coherency and Relationships of TRI and NDVI

The high levels of common variability determined by PCGA both for TRI and NDVI chronologies are in line with previous observations (Galván and others 2014; Fang and others 2012; Bunn and others 2013; Pesaresi and others 2020; Ivanova and others 2021). We found, however, species-specific differences. The relatively less coherent growth pattern of PISY TRI compared to PISY NDVI might have been caused by the more variable topography of PISY sites (Montpellier and others 2018; Oberhuber and Kofler 2000). Additionally, there was a higher variability in age among PISY sites compared to PCAB, which can affect the common growth signal (Konter and others 2016; Mašek and others 2021). PCAB forests in Šumava Mts. are known for disturbance dynamics (wind throws, bark beetle), which might have caused the relatively high variance in NDVI, even though we had cautiously placed our plots in stable and undisturbed areas of the forest stands. Overall, the growth coherence among both TRI and NDVI was anyway high enough to represent the prevailing common signal since PC1 always captured more than 50% of the variance.

Although it has been shown that correlations between NDVI and TRI increase with a spatial resolution (250 m compared to 8 km; Bhuyan and others 2017), our correlation coefficients between

TRI and NDVI ranged from  $-0.27$  to  $0.50$  (based on a resolution of 30 m), which is comparable to other studies that used lower (250 m) resolution MODIS data (Wang and others 2021; Correa-Díaz and others 2019; Schröder and Körner 2018). It is possible that a resolution of 250 m is high enough to obtain ecologically realistic correlations between TRI and NDVI, while spatially more detailed data do not enhance the signal considerably. This suggests that the general pattern of NDVI, and thus leaf biomass production, is captured even with lower-resolution data (250 m).

Overall, PISY sites, particularly plateaus, showed higher correlations between TRI and NDVI than PCAB, probably due to a common climatic driver (drought) for both biomass proxies. The decline of correlations for PISY from plateaus to slopes and valleys was likely caused by increasing moisture availability along the topographic gradient. At PCAB sites, stem and leaf biomass differed in their climatic signal (Table S6), except for the summer months from June to September, which probably led to the low correlations between PCAB TRI and NDVI. It has been demonstrated that correlations between TRI and NDVI tend to increase toward the margins of a species' climatic niche (Alla and others 2017; Coulthard and others 2017; Liang and others 2009). Although PCAB stands in Šumava Mts. are near the climatic optimum of this species (Mäkinen and others 2002), our PISY stands occur in an area experiencing frequent droughts, which can be even more severe at plateaus with shallow soils. Considering the significant correlations between TRI and NDVI for PISY and the clear influence of topography, NDVI, and digital elevation models could be used to spatially interpolate growth dynamics and thus the intensity of carbon sequestration at a landscape level. For our PCAB sites, where the growth patterns of TRI and NDVI were heterogeneous and free of topographic effects, the spatial extrapolation would be highly uncertain.

### Effects of Climate and Topography on TRI and NDVI

Site topographic categories were distinguished by the second or third principal component for PISY TRI but not for any biomass proxy of PCAB. Climatic conditions reflect topographical characteristics, resulting in topographically varying temperature (slope orientation) and water availability (terrain curvature), which is then recorded in tree rings and NDVI (Rappel and others 2018; Riihimäki and others 2017). PISY sites at plateaus were strongly drought-limited due to high solar

radiation and flat terrain unfavorable for long-term moisture accumulation as previously shown for similar areas in Central Europe (Máková 2008). By contrast, PISY sites in the valleys revealed much less drought limitation and even showed a positive effect of summer temperature, which is likely due to moisture accumulation and a common topographically induced temperature inversion (Čílek 2007). In contrast, site categories of PCAB did not differ in their climatic responses, which is probably due to the generally less climatically limited growth and relatively low topographical variability of Šumava Mts. compared to Kokořínsko hills (Figure 1). The topographically different climatic limitations thus presumably were translated into different growth patterns at each PISY site category; by contrast, the landscape-scale growth variability of PCAB was driven by different effects than site climatic conditions.

Interestingly, the seasonal response pattern of PISY NDVI to SPEI was very similar to that of the tree rings, but it was shifted back by one month. This shift suggests that tree-ring formation lags behind needle production by approximately one month, probably due to the onset of growth occurring first in terminal shoots and leaves and its delay toward the stem base (Petit and others 2018). This relationship might have important implications with respect to a temporal decoupling of carbon assimilation in leaves and carbon sequestration in wood biomass (Teets and others 2022; Kannenberg and others 2022; Anderson-Teixeira and others 2022). Leaf biomass production seems to be influenced by climatic conditions at a different time of the year than xylogenesis. Studies have shown that while carbon assimilation (hence vegetation greenness) may start with temperatures of over 0 °C, the growth of trees is limited by temperatures of 5–6 °C (Fatichi and others 2014). These findings may also explain the lag in climate responses of NDVI and TRI in our study. During drought years, the growth (carbon sink) is interrupted earlier than photosynthesis (carbon assimilation) because of low turgor in cells; therefore, assimilated carbon is stored in non-structural carbohydrates which might be used for root production (Teets and others 2022) or for the growth in the following year. This might explain the high correlations of PISY TRI and the low correlations of PISY NDVI with SPEI in the previous year. Overall, the stronger climatic signal of TRI compared to NDVI suggests that wood formation is more strongly driven by climatic constraints than by the availability of source sugars from leaves (Dow and

others 2022; Cabon and others 2022; Fatichi and others 2014).

The response of PCAB (both biomass proxies) to SPEI was generally weak, most likely because moisture is not a growth-limiting factor in the humid environment of Šumava Mts. However, high moisture availability in the preceding summer caused a decrease in NDVI. This could result from wet and cloudy conditions, which might have caused low photosynthesis rates and consequently less available resources invested in bud formation (Alton 2008). PCAB NDVI was also rather insensitive to temperature, except for positive correlations in the previous August and to a larger extent previous December, which can be associated with suitable conditions for bud formation (August) and favorable conditions for soil processes leading to higher accessibility of nitrogen (Weigel and others 2021).

NDVI showed hardly any significant differences between site categories since it is a generally less climate-sensitive proxy than tree-ring width (Peña-Gallardo and others 2018; Liang and others 2009; Gazol and others 2018a). Adult trees preferably allocate biomass to roots during drought periods, mainly at the expense of the stem (Dybzinski and others 2011; Zhang and others 2015; Sevanto and Dickman 2015). This holds the explanation for NDVI and stem growth topographical patterns for PISY in the drought-limited region of Kokořínsko hills, where PISY exhibited less topographical differences of NDVI compared to tree rings. During droughts, trees probably adjusted their biomass allocation at plateaus, while the allocation remained unaffected in valleys. With this, our results suggest that toward the moisture-limited part of the species range, the limitation of sink processes becomes important (Cabon and others 2022). In dry years, the sugar investments in leaves remain less affected and thus the potential intensity of photosynthesis is also not reduced. However, the investment of sugars into stem growth is depressed because cambial cell expansion and division need sufficient delivery of water (Cabon and others 2020). Relatively weaker response of leaf biomass to climate was compared to stem wood biomass thus indirectly corroborating outcomes of studies highlighting the importance of not only source but also sink-limitation processes of tree growth (Fatichi and others 2014; Friend and others 2019; Körner 2015).

Furthermore, it was also argued that a stronger climatic sensitivity of tree rings compared to NDVI may result from partial distortion of the spectral signal due to the limited spatial resolution and due

to noise from other vegetation, which can imprint into the resulting pixel values (Gazol and others 2018a). We tried to avoid artifacts due to admixed species by selecting monospecific sites. Also, soil wetness might imprint into the NDVI signal since it influences spectral reflectance (positively for dry soils; Demattê and others 2004). Unfortunately, canopies of PISY growing in an open stand might not fully cover the ground, and consequently, NDVI estimates might be biased by the presence of ground vegetation. Another explanation for the lower sensitivity of NDVI to climate might be that actual meteorological conditions affecting cambium and needles differ because of the height difference and because the crown shelters the stem. It is likely that the importance of topographical variability in terms of temperature effects is lower at 30 m above the ground than at 1.3 m, where the tree core was taken (Kollas and others 2014). Averaging the NDVI into seasonal values (covering the entire vegetation period May–September) might also have influenced the climatic sensitivity of NDVI. However, data at monthly or biweekly resolution (Brehaut and Danby 2018; Correa-Díaz and others 2019; Wu and others 2017; Wang and others 2021) were not available for high-quality Landsat scenes with no cloud cover in our study areas.

## CONCLUSIONS

Relationships between stem (tree-ring width) and leaf biomass (NDVI) and their climatic signals have so far been studied using low-resolution satellite images masking local topographical differences in forest responses to climate. In this study, we analyzed climate-growth responses of tree-ring widths and NDVI for two main Central European species (*P. abies*, and *P. sylvestris*) at a landscape level using high-resolution Landsat data and systematically taking into account topographic differences. We conclude that the link between tree-ring and NDVI chronologies was generally stronger for *P. sylvestris* compared to *P. abies* and reflected a topographical pattern. Climatic responses of tree rings and NDVI significantly differed in areas near the climatic optimum of a species (*P. abies* in Šumava Mts.). On the other hand, the direction of climate responses of tree rings and NDVI for drought-limited *P. sylvestris* in Kokořínsko hills was similar, but the strength of these responses was strongly modulated by the landscape topography. Overall, tree rings showed a closer link to climatic drivers than NDVI for both species, probably due to a combination of effects such as biomass allocation changes during droughts, spectral distortion of remote sensing data,

and different meteorological conditions influencing the stem and crown. Further research is needed to improve our understanding of the decoupling of the climate signal of different tree compartments. This knowledge is important for forecasting climate change effects on the entire above-ground forest biomass and, consequently, on ecosystems and the carbon cycle.

## ACKNOWLEDGEMENTS

We appreciate the permission and help of the administrators of the protected areas Kokořínsko hills and Šumava Mts. to carry out our research. We are grateful to Charles University Grant Agency (GAUK 548120) for the financial support.

## FUNDING

Open access publishing supported by the National Technical Library in Prague. The study was funded by the Charles University Grant Agency (GAUK 548120).

## DATA AVAILABILITY

Tree-ring width data have been uploaded to the International Tree-Ring Data Bank (ITRDB). Codes for NDVI time-series calculation in Google Earth Engine are provided here: PCAB: <https://code.earthengine.google.com/ddb1fc420d3be0f01719effb1facfa2b>, and PISY: <https://code.earthengine.google.com/8a54269c4279d7795aeec9cc5873d109>. All used data (climate, ring width, and NDVI) are freely available for download on GitHub (<https://github.com/JirkaSkaut/Topographic-variability>) including the R script for all calculations and figure drawings.

## Declarations

**Conflict of interest** The authors declare no conflict of interest.

## OPEN ACCESS

This article is licensed under a Creative Commons Attribution 4.0 International License, which permits use, sharing, adaptation, distribution and reproduction in any medium or format, as long as you give appropriate credit to the original author(s) and the source, provide a link to the Creative Commons licence, and indicate if changes were made. The images or other third party material in this article are included in the article's Creative Commons licence, unless indicated otherwise in a credit line to the material. If material is not

included in the article's Creative Commons licence and your intended use is not permitted by statutory regulation or exceeds the permitted use, you will need to obtain permission directly from the copyright holder. To view a copy of this licence, visit <http://creativecommons.org/licenses/by/4.0/>.

## REFERENCES

- Adams HR, Barnard HR, Loomis AK. 2014. Topography alters tree growth-climate relationships in a semi-arid forested catchment. *Ecosphere* 5:1–16.
- Albrecht J. 2003. Českokobudějovicko. In: Mackovčín P, Sedláček M (eds.): *Chráněná území ČR, svazek VIII. Agentura ochrany přírody a krajiny ČR a EkoCentrum Brno, Praha*, 808 pp.
- Alla AQ, Pasho E, Marku V. 2017. Growth variability and contrasting climatic responses of two *Quercus macrolepis* stands from Southern Albania. *Trees - Struct Funct* 31:1491–1504.
- Alton PB. 2008. Reduced carbon sequestration in terrestrial ecosystems under overcast skies compared to clear skies. *Agric for Meteorol* 148:1641–1653.
- Anderegg WRL, Berry JA, Smith DD, Sperry JS, Anderegg LDL, Field CB. 2012. The roles of hydraulic and carbon stress in a widespread climate-induced forest die-off. *Proc Natl Acad Sci U S A* 109:233–237.
- Anderegg WRL, Schwalm C, Biondi F, Camarero JJ, Koch G, Litvak M, Ogle K, Shaw JD, Shevliakova E, Williams AP, Wolf A, Ziaco E, Pacala S. 2015. Pervasive drought legacies in forest ecosystems and their implications for carbon cycle models. *Science* (80- ) 349:528–32.
- Anderson-Teixeira KJ, Kannenberg SA. 2022. What drives forest carbon storage? The ramifications of source–sink decoupling. *New Phytol* 236:5–8.
- Tolasz R (ed.). 2007. *Atlas podnebí Česka*. ČHMÚ, Praha, Olomouc, 255 s.
- Babst F, Alexander MR, Szejner P, Bouriaud O, Klesse S, Roden J, Ciais P, Poulter B, Frank D, Moore DJP, Trouet V. 2014. A tree-ring perspective on the terrestrial carbon cycle. *Oecologia* 176:307–322.
- Babst F, Poulter B, Bodesheim P, Mahecha MD, Frank DC. 2017. Improved tree-ring archives will support earth-system science. *Nat Ecol Evol* 1:1–2. <https://doi.org/10.1038/s41559-016-0008>.
- Babst F, Bodesheim P, Charney N, Friend AD, Girardin MP, Klesse S, Moore DJP, Seftigen K, Björklund J, Bouriaud O, Dawson A, DeRose RJ, Dietze MC, Eckes AH, Enquist B, Frank DC, Mahecha MD, Poulter B, Record S, Trouet V, Turton RH, Zhang Z, Evans MEK. 2018. When tree rings go global: Challenges and opportunities for retro- and prospective insight. *Quat Sci Rev* 197:1–20.
- Beck PSA, Andreu-Hayles L, D'Arrigo R, Anchukaitis KJ, Tucker CJ, Pinzón JE, Goetz SJ. 2013. A large-scale coherent signal of canopy status in maximum latewood density of tree rings at arctic treeline in North America. *Glob Planet Change* 100:109–118. <https://doi.org/10.1016/j.gloplacha.2012.10.005>.
- Beguéría S, Vicente-Serrano SM. (2017). SPEI: Calculation of the Standardised Precipitation-Evapotranspiration Index. R package version 1.7. <https://CRAN.R-project.org/package=SPEI>
- Berner LT, Beck PSA, Bunn AG, Lloyd AH, Goetz SJ. 2011. High-latitude tree growth and satellite vegetation indices: Correlations and trends in Russia and Canada (1982–2008). *J Geophys Res Biogeosciences* 116:1–13.
- Berner LT, Beck PSA, Bunn AG, Goetz SJ. 2013. Plant response to climate change along the forest-tundra ecotone in north-eastern Siberia. *Glob Chang Biol* 19:3449–3462.
- Bernoulli M, Körner C. 1999. Dry matter allocation in treeline trees. *Phyt - Ann Rei Bot* 39:7–12.
- Beven KJ, Kirkby MJ. 1979. A physically based, variable contributing area model of basin hydrology. *Hydrol. Sci. Bull.* 24:43–69. <https://doi.org/10.1080/02626667909491834>.
- Bhuyan U, Zang C, Vicente-Serrano SM, Menzel A. 2017. Exploring relationships among tree-ring growth, climate variability, and seasonal leaf activity on varying timescales and spatial resolutions. *Remote Sens* 9.
- Břina J, Demek J (2012) *Z nížin do hor: Geomorfologické jednotky České republiky*. Academia Praha. ISBN: 978-802-0020-260, 343s
- Brehaut L, Danby RK. 2018. Inconsistent relationships between annual tree ring-widths and satellite-measured NDVI in a mountainous subarctic environment. *Ecol Indic* 91:698–711. <https://doi.org/10.1016/j.ecolind.2018.04.052>.
- Bunn AG. 2008. A dendrochronology program library in R (dplR). *Dendrochronologia* 26:115–124.
- Bunn AG, Hughes MK, Kirilyanov A V., Losleben M, Shishov V V., Berner LT, Oltchev A, Vaganov EA. 2013. Comparing forest measurements from tree rings and a space-based index of vegetation activity in Siberia. *Environ Res Lett* 8.
- Buras A, Van Der Maaten-Theunissen M, Van Der Maaten E, Ahlgrimm S, Hermann P, Simard S, Heinrich I, Helle G, Unterseher M, Schnittler M, Eusemann P, Wilmking M. 2016. Tuning the voices of a choir: Detecting ecological gradients in time-series populations. *PLoS One* 11:1–21.
- Cabon A, Peters RL, Fonti P, Martínez-Vilalta J, De Cáceres M. 2020. Temperature and water potential co-limit stem cambial activity along a steep elevational gradient. *New Phytol* 226:1325–1340.
- Cabon A, Kannenberg SA, Arain A, Babst F, Baldocchi D, Belmecheri S, Delpierre N, Guerrieri R, Maxwell JT, McKenzie S, Meinzer FC, Moore DJP, Pappas C, Rocha A V., Szejner P, Ueyama M, Ulrich D, Vincke C, Voelker SL, Wei J, Woodruff D, Anderegg WRL. 2022. Cross-biome synthesis of source versus sink limits to tree growth. *Science* (80- ) 761:758–61.
- Carrer M, Urbinati C. 2004. Age-Dependent Tree-Ring Growth Responses to Climate in *Larix decidua* and *Pinus cembra* Author(s): Marco Carrer and Carlo Urbinati Published by: Wiley Stabl URL: <http://www.jstor.org/stable/3450399> REFERENCES Linked references are available on JSTOR f. Ecology 85:730–40.
- Cílek V. 2007. Climate, microclimate and paleoclimate of sandstone areas of Central and Northern Bohemia (Czech republic). In: Härtel H, Cílek V, Herben T, Jackson A, Williams R (eds.): *Sandstone landscapes*. Academia, Praha, s. 97–103.
- Cook E, Peters K. 1981. The smoothing spline, a new approach to standardising forest interior tree-ring. *Trre-Ring Bull* 41:45–53.
- Correa-Díaz A, Silva LCR, Horwath WR, Gómez-Guerrero A, Vargas-Hernández J, Villanueva-Díaz J, Velázquez-Martínez A, Suárez-Espinoza J. 2019. Linking Remote Sensing and Dendrochronology to Quantify Climate-Induced Shifts in High-Elevation Forests Over Space and Time. *J Geophys Res Biogeosciences* 124:166–183.

- Coulthard BL, Touchan R, Anchukaitis KJ, Meko DM, Sivrikaya F. 2017. Tree growth and vegetation activity at the ecosystem-scale in the eastern Mediterranean. *Environ Res Lett* 12.
- ČÚZK (Czech Office for Surveying, Mapping and Cadastre), 2013. Digitální model reliéfu ČR 4. generace.
- D'Arrigo RD, Jacoby GC, Bunker DE, Malmstrom CM, Los SO. 2000. Correlation between maximum latewood density of annual tree rings and NDVI based estimates of forest productivity. *Int J Remote Sens* 21:2329–2336.
- D'Arrigo R, Wilson R, Jacoby G. 2006. On the long-term context for late twentieth century warming. *J Geophys Res Atmos* 111:1–12.
- del Castillo J, Voltas J, Ferrio JP. 2015. Carbon isotope discrimination, radial growth, and NDVI share spatiotemporal responses to precipitation in Aleppo pine. *Trees - Struct Funct* 29:223–233.
- Del-Toro-Guerrero FJ, Kretschmar T, Bullock SH. 2019. Precipitation and topography modulate vegetation greenness in the mountains of Baja California, México. *Int J Biometeorol* 63:1425–1435.
- Dematté JAM, Campos RC, Alves MC, Fiorio PR, Nanni MR. 2004. Visible-NIR reflectance: A new approach on soil evaluation. *Geoderma* 121:95–112.
- Demek J, Balatka B, Czudek T, Láznicka Z, Linhart J, Loučková J, Panoš V, Raušer J, Seichterová H, Sládek J, Stehlík O, Štecl O, Vlček V. 1965. Geomorfologie českých zemí. Nakladatelství Československé akademie věd, Praha, 335 s.
- Donohue RJ, Roderick ML, McVicar TR, Farquhar GD. 2013. Impact of CO<sub>2</sub> fertilization on maximum foliage cover across the globe's warm, arid environments. *Geophys Res Lett* 40:3031–3035.
- Dow C, Kim AY, D'Orangeville L, Gonzalez-Akre EB, Helcoski R, Herrmann V, Harley GL, Maxwell JT, McGregor IR, McShea WJ, McMahon SM, Pederson N, Tepley AJ, Anderson-Teixeira KJ. 2022. Warm springs alter timing but not total growth of temperate deciduous trees. *Nature* 608:552–557.
- Durrant TH, de Rigo D, Caudullo G. 2016. *P. sylvestris* in Europe: distribution, habitat, usage and threats. In: San-Miguel-Ayanz J, de Rigo D, Caudullo G, Houston Durrant T, Mauri A. (Eds.). 2016. European Atlas of Forest Tree Species. Publication Office of the European Union, Luxembourg.
- Dybzinski R, Farrior C, Wolf A, Reich PB, Pacala SW. 2011. Evolutionarily stable strategy carbon allocation to foliage, wood, and fine roots in trees competing for light and nitrogen: An analytically tractable, individual-based model and quantitative comparisons to data. *Am Nat* 177:153–166.
- ESRI, 2020. ArcGIS Desktop: Release 10.7.1. Redlands. Environmental Systems Research Institute, CA.
- Etzold S, Sterck F, Bose AK, Braun S, Buchmann N, Eugster W, Gessler A, Kahmen A, Peters RL, Vitasse Y, Walthert L, Ziemnińska K, Zweifel R. 2022. Number of growth days and not length of the growth period determines radial stem growth of temperate trees. *Ecol Lett* 25:427–439.
- Fajstavr M, Bednářová E, Nezval O, Giagli K, Gryc V, Vavrčík H, Horáček P, Urban J. 2019. How needle phenology indicates the changes of xylem cell formation during drought stress in *P. sylvestris* L. *Dendrochronologia* 56.
- Fang K, Gou X, Chen F, Li Y, Zhang F, Kazmer M. 2012. Tree growth and its association with climate between individual tree-ring series at three mountain ranges in north central China. *Dendrochronologia* 30:113–119. <https://doi.org/10.1016/j.dendro.2011.04.003>.
- Faticchi S, Leuzinger S, Körner C. 2014. Moving beyond photosynthesis: From carbon source to sink-driven vegetation modeling. *New Phytol* 201:1086–1095.
- Friend AD, Patrick AHE, Tim F, Rathgeber CBK, Richardson AD, Turton RH. 2019. On the need to consider wood formation processes in global vegetation models and a suggested approach. *Ann for Sci* 76:49.
- Fritzt HC. 1976. *Tree Rings and Climate*. New York: Academic Press.
- Galván JD, Camarero JJ, Gutiérrez E. 2014. Seeing the trees for the forest: Drivers of individual growth responses to climate in *Pinus uncinata* mountain forests. *J Ecol* 102:1244–1257.
- Gazol A, Camarero JJ, Vicente-Serrano SM, Sánchez-Salguero R, Gutiérrez E, de Luis M, Sangüesa-Barreda G, Novak K, Rozas V, Tiscar PA, Linares JC, Martín-Hernández N, Martínez del Castillo E, Ribas M, García-González I, Silla F, Camisón A, Génova M, Olano JM, Longares LA, Hevia A, Tomás-Burguera M, Galván JD. 2018a. Forest resilience to drought varies across biomes. *Glob Chang Biol* 24:2143–2158.
- Gazol A, Camarero JJ, Sangüesa-Barreda G, Vicente-Serrano SM. 2018b. Post-drought resilience after forest die-off: Shifts in regeneration, composition, growth and productivity. *Front Plant Sci* 871:1–12.
- Girardin MP, Bouriaud O, Hogg EH, Kurz W, Zimmermann NE, Metsaranta JM, De Jong R, Frank DC, Esper J, Büntgen U, Guo XJ, Bhatti J. 2016. No growth stimulation of Canada's boreal forest under half-century of combined warming and CO<sub>2</sub> fertilization. *Proc Natl Acad Sci U S A* 113:E8406–E8414.
- Gorelick N, Hancher M, Dixon M, Ilyushchenko S, Thau D, Moore R. 2017. Google Earth Engine: Planetary-scale geospatial analysis for everyone. *Remote Sens Environ* 202:18–27. <https://doi.org/10.1016/j.rse.2017.06.031>.
- Hájková L (ed.). 2012. Atlas fenologických poměrů Česka. Praha: Český hydrometeorologický ústav; Olomouc, 2012. ISBN 978–80–86690–98–8.
- Instruments Regent. 2011. WinDendro Image Analysis System. Québec: Regent Instruments Inc.
- Ivanova Y, Kovalev A, Soukhovolsky V. 2021. Modeling the radial stem growth of the pine (*P. sylvestris* l.) forests using the satellite-derived ndvi and lst (modis/aqua) data. *Atmosphere (basel)* 12:1–15.
- Kannenberg SA, Novick KA, Alexander MR, Maxwell JT, Moore DJP, Phillips RP, Anderegg WRL. 2019. Linking drought legacy effects across scales: From leaves to tree rings to ecosystems. *Glob Chang Biol* 25:2978–2992.
- Kannenberg SA, Cabon A, Babst F, Belmecheri S, Delpierre N, Guerrieri R, Maxwell JT, Meinzer FC, Moore DJP, Pappas C, Ueyama M, Ulrich DEM, Voelker SL, Woodruff DR, Anderegg WRL. 2022. Drought-induced decoupling between carbon uptake and tree growth impacts forest carbon turnover time. *Agric For Meteorol* 322:108996. <https://doi.org/10.1016/j.agrfor.2022.108996>
- Kaufmann RK, D'Arrigo RD, Paletta LF, Tian HQ, Jolly WM, Myneni RB. 2008. Identifying climatic controls on ring width: The timing of correlations between tree rings and NDVI. *Earth Interact* 12:1–14.
- Knibbe B. 2004. *Personal Analysis System for Tree-ring Research 4 - Instruction Manual*. Vienna: SCIEIM.
- Kollas C, Randin CF, Vitasse Y, Körner C. 2014. How accurately can minimum temperatures at the cold limits of tree species be extrapolated from weather station data? *Agric for Meteorol*

- 184:257–266. <https://doi.org/10.1016/j.agrformet.2013.10.001>.
- Konter O, Büntgen U, Carrer M, Timonen M, Esper J. 2016. Climate signal age effects in boreal tree-rings: Lessons to be learned for paleoclimatic reconstructions. *Quat Sci Rev* 142:164–172. <https://doi.org/10.1016/j.quascirev.2016.04.020>.
- Körner C. 2015. Paradigm shift in plant growth control. *Curr Opin Plant Biol* 25:107–114.
- Kraus C, Zang C, Menzel A. 2016. Elevational response in leaf and xylem phenology reveals different prolongation of growing period of common beech and Norway spruce under warming conditions in the Bavarian Alps. *Eur J for Res* 135:1011–1023.
- Krejza J, Cienciala E, Světlík J, Bellan M, Noyer E, Horáček P, Štěpánek P, Marek MV. 2021. Evidence of climate-induced stress of Norway spruce along elevation gradient preceding the current dieback in Central Europe. *Trees - Struct Funct* 35:103–119. <https://doi.org/10.1007/s00468-020-02022-6>.
- Le Quéré C, Raupach MR, Canadell JG, Marland G, Bopp L, Ciais P, Conway TJ, Doney SC, Feely RA, Foster P, Friedlingstein P, Gurney K, Houghton RA, House JI, Huntingford C, Levy PE, Lomas MR, Majkut J, Metz N, Ometto JP, Peters GP, Prentice IC, Randerson JT, Running SW, Sarmiento JL, Schuster U, Sitch S, Takahashi T, Viovy N, Van Der Werf GR, Woodward FI. 2009. Trends in the sources and sinks of carbon dioxide. *Nat Geosci* 2:831–836.
- Leavitt SW, Chase TN, Rajagopalan B, Lee E, Lawrence PJ. 2008. Southwestern U.S. tree-ring carbon isotope indices as a possible proxy for reconstruction of greenness of vegetation. *Geophys Res Lett* 35:1–5.
- Liang EY, Shao XM, He JC. 2005. Relationships between tree growth and NDVI of grassland in the semi-arid grassland of north China. *Int J Remote Sens* 26:2901–2908.
- Liang E, Eckstein D, Liu H. 2009. Assessing the recent grassland greening trend in a long-term context based on tree-ring analysis: A case study in North China. *Ecol Indic* 9:1280–1283.
- Lopatin E, Kolström T, Spiecker H. 2006. Determination of forest growth trends in Komi Republic (northwestern Russia): Combination of tree-ring analysis and remote sensing data. *Boreal Environ Res* 11:341–353.
- Ložek V, Kubíková J, Spryňar P. 2005. Střední Čechy. In: Mackovčín P, Sedláček M (eds.): *Chráněná území ČR, svazek XIII. Agentura ochrany přírody a krajiny ČR a EkoCentrum Brno, Praha*, 904 pp.
- Lu GY, Wong DW. 2008. An adaptive inverse-distance weighting spatial interpolation technique. *Comput Geosci* 34:1044–1055.
- Mácová M. 2008. Dendroclimatological comparison of native *P. sylvestris* and invasive *Pinus strobus* in different habitats in the Czech Republic. *Preslia* 80:277–289.
- Mäkinen H, Nöjd P, Kahle HP, Neumann U, Tveite B, Mielikäinen K, Röhle H, Spiecker H. 2002. Radial growth variation of Norway spruce (*P. abies* (L.) Karst.) across latitudinal and altitudinal gradients in central and northern Europe. *For Ecol Manage* 171:243–259.
- Mašek J, Tumajer J, Rydval M, Lange J, Tremel V. 2021. Age and size outperform topographic effects on growth-climate responses of trees in two Central European coniferous forest types. *Dendrochronologia* 68:125845.
- Montpellier EE, Soulé PT, Knapp PA, Shelly JS. 2018. Divergent growth rates of alpine larch trees (*Larix lyallii* Parl.) in response to microenvironmental variability. *Arctic, Antarct Alp Res* 50:1–9. <https://doi.org/10.1080/15230430.2017.1415626>.
- NASA. 2022. Measuring vegetation NDVI & EVI. Normalized Difference Vegetation Index (NDVI). [http://earthobservatory.nasa.gov/Features/MeasuringVegetation/measuring\\_vegetation\\_on\\_2.php](http://earthobservatory.nasa.gov/Features/MeasuringVegetation/measuring_vegetation_on_2.php) (12.5.2022)
- Oberhuber W, Kofler W. 2000. Topographic influences on radial growth of Scots pine (*P. sylvestris* L.) at small spatial scales. *Plant Ecol* 146:231–240.
- Pan Y, Birdsey RA, Fang J, Houghton R, Kauppi PE, Kurz WA, Phillips OL, Shvidenko A, Lewis SL, Canadell JG, Ciais P, Jackson RB, Pacala SW, McGuire AD, Piao S, Rautiainen A, Sitch S, Hayes D. 2011. A large and persistent carbon sink in the world's forests. *Science* 333:988–993.
- Pasho E, Alla AQ. 2015. Climate impacts on radial growth and vegetation activity of two co-existing Mediterranean pine species. *Can J for Res* 45:1748–1756.
- Pebesma EJ. 2004. Multivariable geostatistics in S: The gstat package. *Comput Geosci* 30:683–691.
- Peña-Gallardo M, Vicente-Serrano SM, Camarero JJ, Gazol A, Sánchez-Salguero R, Domínguez-Castro F, El Kenawy A, Beguería-Portugés S, Gutiérrez E, de Luis M, Sangüesa-Barreda G, Novak K, Rozas V, Tíscar PA, Linares JC, del Castillo EM, Matamoros MR, García-González I, Silla F, Camisón Á, Génova M, Olano JM, Longares LA, Hevia A, Galván JD. 2018. Drought sensitiveness on forest growth in peninsular Spain and the Balearic Islands. *Forests* 9:1–20.
- Pesaresi S, Mancini A, Quattrini G, Casavecchia S. 2020. Mapping mediterranean forest plant associations and habitats with functional principal component analysis using Landsat 8 NDVI time series. *Remote Sens* 12.
- Petit G, von Arx G, Kiorapostolou N, Lechthaler S, Prendin AL, Anfodillo T, Caldeira MC, Cochard H, Copini P, Crivellaro A, Delzon S, Gebauer R, Gričar J, Grönholm L, Hölttä T, Jyske T, Lavrič M, Lintunen A, Lobo-do-Vale R, Peltoniemi M, Peters RL, Robert EMR, Roig Juan S, Senfeldt M, Steppe K, Urban J, Van Camp J, Sterck F. 2018. Tree differences in primary and secondary growth drive convergent scaling in leaf area to sapwood area across Europe. *New Phytol* 218:1383–1392.
- Pompa-García M, Camarero JJ, Colangelo M, González-Cásares M. 2021. Inter and intra-annual links between climate, tree growth and NDVI: improving the resolution of drought proxies in conifer forests. *Int J Biometeorol* 65:2111–2121. <https://doi.org/10.1007/s00484-021-02170-5>.
- Ponocná T, Spyt B, Kaczka R, Büntgen U, Tremel V. 2016. Growth trends and climate responses of Norway spruce along elevational gradients in East-Central Europe. *Trees - Struct Funct* 30:1633–1646.
- R Core Team. 2019. R: A language and environment for statistical computing. R Foundation for Statistical Computing, Vienna, Austria. URL <https://www.R-project.org/>.
- Rabbel I, Neuwirth B, Bogena H, Diekkrüger B. 2018. Exploring the growth response of Norway spruce (*P. abies*) along a small-scale gradient of soil water supply. *Dendrochronologia* 52:123–130. <https://doi.org/10.1016/j.dendro.2018.10.007>.
- Riihimäki H, Heiskanen J, Luoto M. 2017. The effect of topography on arctic-alpine aboveground biomass and NDVI patterns. *Int J Appl Earth Obs Geoinf* 56:44–53. <https://doi.org/10.1016/j.jag.2016.11.005>.
- Roy DP, Kovalsky V, Zhang HK, Vermote EF, Yan L, Kumar SS, Egorov A. 2016. Characterization of Landsat-7 to Landsat-8 reflective wavelength and normalized difference vegetation index continuity. *Remote Sens Environ* 185:57–70.

- Schroeder J, Körner M. 2018. Remote-sensing data are closely related to growth information in tree-ring index chronologies. TRACE—Tree Rings Archaeol Climatol Ecol Vol 7 Proc DENDROSYMPOSIUM 2008, April 27th–30th 2008. Zakopane, Poland 16:14–24.
- Seftigen K, Frank DC, Björklund J, Babst F, Poulter B. 2018. The climatic drivers of normalized difference vegetation index and tree-ring-based estimates of forest productivity are spatially coherent but temporally decoupled in Northern Hemispheric forests. *Glob Ecol Biogeogr* 27:1352–1365.
- Sevanto S, Dickman LT. 2015. Where does the carbon go?—Plant carbon allocation under climate change. *Tree Physiol* 35:581–584.
- Shabanov NV, Huang D, Yang W, Tan B, Knyazikhin Y, Myneni RB, Ahl DE, Gower ST, Huete AR, Aragão LEOC, Shimabukuro YE. 2005. Analysis and optimization of the MODIS leaf area index algorithm retrievals over broadleaf forests. *IEEE Trans Geosci Remote Sens* 43:1855–1865.
- Song C. 2012. Optical remote sensing of forest leaf area index and biomass. *Prog Phys Geogr* 37:98–113.
- Spiecker H. 2000. Spruce monocultures in Central Europe – Problems and prospects (Issue 33). European Forest Institute.
- Sprenger M, Stump C, Weiler M, Aeschbach W, Allen ST, Benettin P, Dubbert M, Hartmann A, Hrachowitz M, Kirchner JW, McDonnell JJ, Orlowski N, Penna D, Pfahl S, Rinderer M, Rodriguez N, Schmidt M, Werner C. 2019. The Demographics of Water: A Review of Water Ages in the Critical Zone. *Rev Geophys* 57:800–834.
- Teets A, Moore DJP, Alexander MR, Blanken PD, Bohrer G, Burns SP, Carbone MS, Ducey MJ, Fraver S, Gough CM, Hollinger DY, Koch G, Kolb T, Munger JW, Novick KA, Ollinger SV, Ouimette AP, Pederson N, Ricciuto DM, Seydinasrollah B, Vogel CS, Richardson AD. 2022. Coupling of Tree Growth and Photosynthetic Carbon Uptake Across Six North American Forests. *J Geophys Res Biogeosciences* 127:1–20.
- Thornthwaite CW. 1948. An Approach toward a Rational Classification of Climate. *Geogr Rev* 38:55.
- Tumajer J, Scharnweber T, Smiljanic M, Wilmking M. 2022. Limitation by vapour pressure deficit shapes different intra-annual growth patterns of diffuse- and ring-porous temperate broadleaves. *New Phytol* 233:2429–2441.
- Vicente-Serrano SM, Lasanta T, Romo A. 2004. Analysis of spatial and temporal evolution of vegetation cover in the Spanish central pyrenees: Role of human management. *Environ Manage* 34:802–818.
- Vicente-Serrano SM, Beguería S, López-Moreno JI. 2010. A multiscale drought index sensitive to global warming: The standardized precipitation evapotranspiration index. *J Clim* 23:1696–1718.
- Vicente-Serrano SM, Gouveia C, Camarero JJ, Beguería S, Trigo R, López-Moreno JI, Azorín-Molina C, Pasho E, Lorenzo-Lacruz J, Revuelto J, Morán-Tejeda E, Sanchez-Lorenzo A. 2012. Response of vegetation to drought time-scales across global land biomes. *Proc Natl Acad Sci U S A* 110:52–57.
- Vicente-Serrano SM, Camarero JJ, Olano JM, Martín-Hernández N, Peña-Gallardo M, Tomás-Burguera M, Gazol A, Azorín-Molina C, Bhuyan U, El Kenawy A. 2016. Diverse relationships between forest growth and the Normalized Difference Vegetation Index at a global scale. *Remote Sens Environ* 187:14–29. <https://doi.org/10.1016/j.rse.2016.10.001>.
- Vicente-Serrano SM, Martín-Hernández N, Camarero JJ, Gazol A, Sánchez-Salguero R, Peña-Gallardo M, El Kenawy A, Domínguez-Castro F, Tomás-Burguera M, Gutiérrez E, de Luis M, Sangüesa-Barreda G, Novak K, Rozas V, Tiscar PA, Linares JC, del Castillo EM, Ribas M, García-González I, Silla F, Camisón A, Génova M, Olano JM, Longares LA, Hevia A, Diego Galván J. 2020. Linking tree-ring growth and satellite-derived gross primary growth in multiple forest biomes. Temporal-scale matters. *Ecol Indic* 108:105753. <https://doi.org/10.1016/j.ecolind.2019.105753>
- Wang J, Rich PM, Price KP, Kettle WD. 2004. Relations between NDVI and tree productivity in the central Great Plains. *Int J Remote Sens* 25:3127–3138.
- Wang Z, Lyu L, Liu W, Liang H, Huang J, Zhang Q Bin. 2021. Topographic patterns of forest decline as detected from tree rings and NDVI. *Catena* 198:105011. <https://doi.org/10.1016/j.catena.2020.105011>
- Weigel R, Henry HAL, Beil I, Gebauer G, Jurasinski G, Klisz M, van der Maaten E, Muffler L, Kreyling J. 2021. Ecosystem Processes Show Uniform Sensitivity to Winter Soil Temperature Change Across a Gradient from Central to Cold Marginal Stands of a Major Temperate Forest Tree. *Ecosystems* 24:1545–1560. <https://doi.org/10.1007/s10021-021-00600-4>.
- Wong CYS, Young DJN, Latimer AM, Buckley TN, Magney TS. 2021. Importance of the legacy effect for assessing spatiotemporal correspondence between interannual tree-ring width and remote sensing products in the Sierra Nevada. *Remote Sens Environ* 265:112635. <https://doi.org/10.1016/j.rse.2021.112635>
- Wu X, Liu H, Li X, Ciais P, Babst F, Guo W, Zhang C, Magliulo V, Pavelka M, Liu S, Huang Y, Wang P, Shi C, Ma Y. 2017. Differentiating drought legacy effects on vegetation growth over the temperate Northern Hemisphere. *Glob Chang Biol* 24:504–516.
- Xu P, Fang W, Zhou T, Zhao X, Luo H, Hendrey G, Yi C. 2019. Spatial upscaling of tree-ring-based forest response to drought with satellite data. *Remote Sens* 11:16–18.
- Zang C, Biondi F. 2015. Treeclim: An R package for the numerical calibration of proxy-climate relationships. *Ecography (cop)* 38:431–436.
- Zhan Z-Z, Liu H-B, Li H-M, Wu W, Zhong B. 2012. The Relationship between NDVI and Terrain Factors—A Case Study of Chongqing. *Procedia Environ Sci* 12:765–771. <https://doi.org/10.1016/j.proenv.2012.01.347>.
- Zhang H, Wang K, Xu X, Song T, Xu Y, Zeng F. 2015. Biogeographical patterns of biomass allocation in leaves, stems, and roots in China's forests. *Sci Rep* 5:1–12.
- Zhang T, Zhang R, Lu B, Mambetov BT, Kelgenbayev N, Dosmanbetov D, Maisupova B, Chen F, Yu S, Shang H, Huang L. 2018. *Picea schrenkiana* tree-ring chronologies development and vegetation index reconstruction for the Alatau Mountains, Central Asia. *Geochronometria* 45:107–118.
- Zhu Z, Wang S, Woodcock CE. 2015. Improvement and expansion of the Fmask algorithm: Cloud, cloud shadow, and snow detection for Landsats 4–7, 8, and Sentinel 2 images. *Remote Sens Environ* 159:269–277. <https://doi.org/10.1016/j.rse.2014.12.014>.